International Journal of Thermophysics, Vol. 13, No. 4, 1992

Thermodynamic Properties of Methane in the Critical Region

G. X. Jin,[1] S. Tang,[1] and J. V. Sengers[1,2]

Received February 18, 1992

An equation of state is presented for the thermodynamic properties of methane in the vicinity of the critical point. It incorporates the scaled asymptotic critical behavior predicted theoretically and supplements a global analytic equation of state for methane recently developed by Setzmann and Wagner.

KEY WORDS: coexistence curve; critical phenomena; equation of state; methane; sound velocity; specific heat; thermodynamic properties.

1. INTRODUCTION

It has been well established from theory and experiment that the thermodynamic surface of fluids has a singularity near the critical point [1]. This singularity can be characterized in terms of asymptotic scaling laws with universal critical exponents and universal scaling functions [2, 3]. The asymptotic scaling laws can be extended by including leading confluent singularities, known as correction-to-scaling terms, and by revising the scaling fields to account for vapor–liquid asymmetry [2, 4].

A major problem has been how to incorporate the singular behavior near the critical point into a global thermodynamic surface that remains analytic at the critical point [3]. This problem was first addressed by Chapela and Rowlinson [5], who tried to represent the equations of state for carbon dioxide and methane as a sum of a scaled equation and an analytic equation with weights determined by a switching function. However, it turns out that a switching function leads to abnormal behavior

[1] Institute for Physical Science and Technology, University of Maryland, College Park, Maryland 20742, U.S.A.

[2] Thermophysics Division, National Institute of Standards and Technology, Technology Administration, U.S. Department of Commerce, Gaithersburg, Maryland 20899, U.S.A.

0195-928X/92/0700-0671$06.50/0

of thermodynamic properties that involve derivatives of the equation of state [6, 7]. Therefore, when Angus et al. [8] developed an equation of state for methane under the sponsorship of IUPAC, the attempt to combine the global analytic equation of state with a scaled equation of state near the critical point was abandoned. As a consequence, in specifying the range of validity of the IUPAC equation of state for methane, a region around the critical point had to be excluded.

An attempt to remedy this limitation was made by Kurumov and co-workers [9], who represented the thermodynamic properties of methane near the critical point in terms of a parametric scaled equation of state originally proposed by Balfour et al. [4] and subsequently applied to many fluids [2]. To obtain consistency with the global IUPAC formulation, Kurumov et al. determined the coefficients in their scaled equation of state by fitting not exclusively to experimental thermodynamic-property data but by including also values calculated from the IUPAC formulation. Unfortunately, the attempt of Kurumov et al. was only partially successful. The problem was that the range of validity of the scaled equation was not large enough to accomplish a smooth connection with the global IUPAC formulation. As a consequence Kurumov et al. were forced to conclude that "there are ranges of densities where neither the scaled fundamental equation nor the IUPAC formulation yields a satisfactory representation of the thermodynamic surface" [9].

In recent years several investigators have tried to develop improved equations for the Helmholtz free energy of methane as a function of density and temperature [10–12]. Brandani and Prausnitz [10] had earlier shown that by adding some simple correction functions to a Helmholtz free energy implied by a generalized Redlich–Kwong equation considerable improvement in the critical region can be achieved. New comprehensive fundamental equations for methane have been proposed by Friend et al. [11] and by Setzmann and Wagner [12]. The latter two equations are substantial improvements over the previous IUPAC formulation. Among the equations of state for methane mentioned above the equation of Setzmann and Wagner appears to be the most accurate one. In developing this new equation of state an extensive set of experimental data was used [13–15] that was not available at the time that the earlier IUPAC formulation was constructed. Moreover, by using not only the coefficients, but also the powers of temperature and density in the equation as adjustable system-dependent variables, Setzmann and Wagner were able to extend their global equation for methane into the critical region that was excluded in the IUPAC formulation.

This equation of Setzmann and Wagner yields an accurate representation of the thermodynamic properties of methane suitable for all practical

applications. Nevertheless, the equation of state of Setzmann and Wagner, as is also the case with the other global equations, remains analytic at the critical point and consequently fails to account for the singular thermodynamic behavior at the critical point such as a divergent behavior of the specific heat [16]. For scientific use we need an equation of state in the near-vicinity of the critical point that incorporates the asymptotic critical scaling laws. In this paper we present an equation of state for methane near the critical point that supplements the global equation of Setzmann and Wagner. It is based on a new theoretical equation of state for fluids in the critical region that not only includes the scaled behavior asymptotically close to the critical point, but also accounts for the crossover to analytic behavior away from the critical point [17–19]. The equation presented in this paper for methane near the critical point replaces the scaled equation of state earlier presented by Kurumov et al. [9].

2. HELMHOLTZ FREE-ENERGY DENSITY IN THE CRITICAL REGION

Our formulation is based on a crossover equation for the Helmholtz free-energy density, i.e., the Helmholtz free energy A per unit of volume V. Specifically, we use the six-term Landau crossover model derived by Chen and co-workers [18]. The asymptotic critical behavior of this crossover model has been further analyzed by Tang et al. [19]. The equation of state used in this paper corresponds to the version designated by Tang et al. as "crossover model II."

Let T be the temperature, P the pressure, ρ the density, and μ the chemical potential. We use the critical temperature T_c, the critical pressure P_c, and the critical density ρ_c to define dimensionless properties as

$$\tilde{T} = -\frac{T_c}{T}, \qquad \tilde{\rho} = \frac{\rho}{\rho_c}, \qquad \tilde{\mu} = \frac{\rho_c T_c}{P_c}\frac{\mu}{T}, \qquad \tilde{A} = \frac{T_c}{P_c}\frac{A}{VT} \tag{1}$$

The Helmholtz free-energy density $\tilde{A}$ is decomposed as

$$\tilde{A} = \Delta\tilde{A} + \tilde{\rho}\tilde{\mu}_0(\tilde{T}) + \tilde{A}_0(\tilde{T}) \tag{2}$$

where $\tilde{\mu}_0(\tilde{T})$ and $\tilde{A}_0(\tilde{T})$ are analytic background functions such that $\tilde{A}_0 = -1$ at the critical temperature. The term $\Delta\tilde{A}$ in Eq. (2) contains the singular behavior and is treated as a function of the variables $\Delta\tilde{T}$ and $\Delta\tilde{\rho}$ defined as

$$\Delta\tilde{T} = \tilde{T} + 1, \qquad \Delta\tilde{\rho} = \tilde{\rho} - 1 \tag{3}$$

In the classical theory $\Delta\tilde{A}$ can be expanded around the critical point by a Taylor series of the form [18]

$$\Delta\tilde{A}_{\rm cl}=\frac{1}{2}tM^2+\frac{1}{4!}u\Lambda M^4+\frac{1}{5!}a_{05}M^5 + \frac{1}{6!}a_{06}M^6+\frac{1}{4!}a_{14}tM^4+\frac{1}{2!\,2!}a_{22}t^2M^2 \tag{4}$$

where u, Λ, a_{05}, a_{06}, a_{14}, and a_{22} are system-dependent coefficients. The temperature-like variable t and the order parameter M are related to the physical variables $\Delta\tilde{T}$ and $\Delta\tilde{\rho}$ in a manner specified below. Unlike the three-dimensional Ising model, a fluid is not symmetric in the order parameter M [20]. This lack of symmetry is reflected in the presence of a term proportional to M^5 in the expansion given by Eq. (4).

As shown by Chen et al. [18], a renormalized $\Delta\tilde{A}_{\rm r}$, incorporating the effects of critical fluctuations, can be constructed from Eq. (4) by the following transformation:

(i) replace the variable t by $t\mathscr{T}\mathscr{U}^{-1/2}$,

(ii) replace the variable M in the even terms by $M\mathscr{D}^{1/2}\mathscr{U}^{1/4}$ and in the odd M^5 term by $M\mathscr{D}^{1/2}\mathscr{U}^{1/5}\mathscr{V}^{1/5}$, and

(iii) add a fluctuation-induced additional contribution $-\frac{1}{2}t^2\mathscr{K}$.

The new functions in the above transformation are defined as

$$\mathscr{T}=Y^{(2\nu-1)/\Delta},\qquad \mathscr{D}=Y^{-\eta\nu/\Delta},\qquad \mathscr{U}=Y^{\nu/\Delta},$$
$$\mathscr{V}=Y^{(\Delta_{\rm a}-\nu/2)/\Delta},\qquad \mathscr{K}=\frac{\nu}{\alpha\bar{u}\Lambda}(Y^{-\alpha/\Delta}-1) \tag{5}$$

where ν, η, α, Δ, and $\Delta_{\rm a}$ are universal critical exponents and where $\bar{u}$ is defined as

$$\bar{u}=u/u^* \tag{6}$$

with u^* being a universal fixed-point coupling constant. For these universal quantities we continue to use the values adopted by Chen et al. [18], and they are reproduced in Table I. The crossover function Y in Eq. (5) is to be determined from [18]

$$1-(1-\bar{u})Y=\bar{u}\left(1+\frac{\Lambda^2}{\kappa^2}\right)^{1/2}Y^{\nu/\Delta} \tag{7}$$

with

$$\kappa^2=t\mathscr{T}+\frac{1}{2}u^*\bar{u}\Lambda M^2\mathscr{D}\mathscr{U} \tag{8}$$

Table I. Universal Constants

$\nu = 0.630$
$\eta = 0.0333$
$\alpha = 2 - 3\nu = 0.110$
$\Delta = 0.51$
$\Delta_a = 1.323$
$u^* = 0.472$

After applying the above transformation to the Landau expansion (4), we obtain

$$\Delta\tilde{A}_r = \frac{1}{2} tM^2\mathscr{T}\mathscr{D} + \frac{1}{4!} u^*\bar{u}\Lambda M^4\mathscr{D}^2\mathscr{U} + \frac{1}{5!} a_{05} M^5\mathscr{D}^{5/2}\mathscr{V}\mathscr{U} + \frac{1}{6!} a_{06} M^6\mathscr{D}^3\mathscr{U}^{3/2}$$

$$+ \frac{1}{4!} a_{14} tM^4\mathscr{T}\mathscr{D}^2\mathscr{U}^{1/2} + \frac{1}{2!\,2!} a_{22} t^2M^2\mathscr{T}^2\mathscr{D}\mathscr{U}^{-1/2} - \frac{1}{2} t^2\mathscr{K} \tag{9}$$

The variable κ^2, defined by Eq. (8), serves as a measure of the distance from the critical point. As $\kappa^2 \to 0$, $Y \to 0$ and one recovers from Eq. (9) the asymptotic critical scaling laws [19]. As $\kappa^2 \to \infty$, $Y \to 1$ and Eq. (9) reduces to the classical Landau expansion given by Eq. (4).

As discussed by Chen et al. [18, 21], the singular Helmholtz free-energy density $\Delta\tilde{A}$ in Eq. (2) is related to $\Delta\tilde{A}_r$ by

$$\Delta\tilde{A} = \Delta\tilde{A}_r - c\left(\frac{\partial\tilde{A}_r}{\partial M}\right)_t \left(\frac{\partial\tilde{A}_r}{\partial t}\right)_M \tag{10}$$

where the coefficient c is a small system-dependent constant related to a lack of vapor–liquid symmetry. The variables t and M in Eq. (9) are related to $\Delta\tilde{T}$ and $\Delta\tilde{\rho}$ by [18, 21]

$$t = c_t\,\Delta\tilde{T} + c\left(\frac{\partial\tilde{A}_r}{\partial M}\right)_t, \qquad M = c_\rho(\Delta\tilde{\rho} - d_1\,\Delta\tilde{T}) + c\left(\frac{\partial\tilde{A}_r}{\partial t}\right)_M \tag{11}$$

where c_t, c_ρ, and d_1 are additional system-dependent coefficients. Finally, to specify the total Helmholtz free-energy density $\tilde{A}$, defined by Eq. (2), we represent the analytic background functions $\tilde{A}_0(\tilde{T})$ and $\tilde{\mu}_0(\tilde{T})$ by truncated Taylor expansions,

$$\tilde{A}_0(\tilde{T}) = -1 + \sum_{j=1}^{4} \tilde{A}_j(\Delta\tilde{T})^j \tag{12}$$

$$\tilde{\mu}_0(\tilde{T}) = \sum_{j=0}^{5} \tilde{\mu}_j(\Delta\tilde{T})^j \tag{13}$$

where $\tilde{A}_j$ and $\tilde{\mu}_j$ are system-dependent coefficients.

The relevant equations needed to calculate the various thermodynamic properties from our crossover model for the Helmholtz free-energy density are given in a previous publication [18]. The computation of the singular part $\Delta\tilde{A}$ the Helmholtz free-energy density for a given temperature T and a given density ρ, proceeds as follows.

(i) Calculate zeroth-order estimates for the variables t and M as $t_0 = c_t \Delta\tilde{T}$ and $M_0 = c_\rho(\Delta\tilde{\rho} - d_1 \Delta\tilde{T})$, respectively.

(ii) Calculate the corresponding values $Y_0 = Y(t_0, M_0)$ and $\kappa_0 = \kappa(t_0, M_0)$ from Eqs. (7) and (8) by iteration.

(iii) Calculate $(\partial \Delta\tilde{A}_r/\partial t)_M$ and $(\partial \Delta\tilde{A}_r/\partial M)_t$ in this approximation and obtain new estimates t_1 and M_1 for t and M from Eq. (11).

(iv) Iterate the procedure until convergence is obtained.

3. APPLICATION TO METHANE

In developing our equation of state for methane in the critical region we converted all temperatures to the new international temperature scale of 1990 [22], as was also done by Setzmann and Wagner [12]. The values reported in the literature for the critical parameters T_c, P_c, and ρ_c of methane have been reviewed by Setzmann and Wagner. They accepted as the most probable values $T_c = 190.564$ K, $P_c = 4.5922$ MPa, and $\rho_c = 162.66\ \text{kg} \cdot \text{m}^{-3}$, which had been obtained by Kleinrahm and Wagner [13] and which had also been retained by Kurumov et al. [9]. For T_c and P_c we continued to use the same values as quoted above. However, we found that our equation of state yielded a better representation of the experimental coexisting vapor and liquid densities near the critical point if the critical density was reduced to $\rho_c = 162.38\ \text{kg} \cdot \text{m}^{-3}$. This small downward shift is probably due to the presence of the asymptotic singular curvature of the coexistence diameter implied by scaled equations of state [16, 18, 23] and which is not present in analytic equations like the one used by Setzmann and Wagner.

In addition to the critical parameters, or crossover model for the Helmholtz free-energy density contains the following system-dependent constants: the crossover constants $\bar{u}$ and Λ, the coefficients c_t, c_ρ, c, and d_1 in the relations given by Eq. (11) between the theoretical and the physical variables, the coefficients a_{ij} of the classical Landau expansion given by Eq. (4), the coefficients $\tilde{A}_j$ in the background contribution to the pressure, and the coefficients $\tilde{\mu}_j$ in the background contribution to the caloric properties. Except for the caloric background coefficients $\tilde{\mu}_j$, these constants can be determined from a fit of our crossover model to experimental

P–ρ–T data [18]. For methane we used the experimental P–ρ–T data obtained by Wagner and co-workers in the one-phase region [14, 15] as well as along the vapor–liquid phase boundary [13]. With $\sigma_P = 0.007\%$, $\sigma_T = 0.001$ K, and $\sigma_\rho = 0.02\%$ as the estimated errors in pressure, temperature, and density for the experimental P–ρ–T data and with the uncertainties as estimated by Kleinrahm and Wagner [13] for the coexistence properties, our crossover equation of state, with the system-dependent coefficients listed in Table II, reproduces these experimental data with a reduced chi-square of 0.53 in a range of densities and temperatures around the critical point bounded by

$$\tilde{\chi}^{-1} \equiv \left(\frac{\partial^2 \Delta\tilde{A}}{\partial \Delta\tilde{\rho}^2}\right)_{\Delta\tilde{T}} \leqslant 1.4 \qquad \text{and} \qquad T \geqslant 186 \text{ K} \tag{14}$$

Table II. System-Dependent Constants for Methane

Critical-point parameters	
T_c	190.564 K (ITS-90)
P_c	4.5992 MPa
ρ_c	162.38 kg · m^{-3}
Crossover parameters	
$\bar{u}$	0.25376
Λ	1.2873
Scaling-field parameters	
c_t	1.2798
c_ρ	2.6165
c	−0.043264
d_1	−0.41063
Classical parameters	
a_{05}	0.052257
a_{06}	0.83670
a_{14}	0.59968
a_{22}	1.0879
Equation-of-state background parameters	
$\tilde{A}_1$	−4.9838
$\tilde{A}_2$	3.2997
$\tilde{A}_3$	1.2843
$\tilde{A}_4$	3.2983
Caloric background parameters	
$\tilde{\mu}_0$	7.291
$\tilde{\mu}_1$	7.188
$\tilde{\mu}_2$	−10.261
$\tilde{\mu}_3$	−4.8579
$\tilde{\mu}_4$	3.5384
$\tilde{\mu}_5$	−43.171

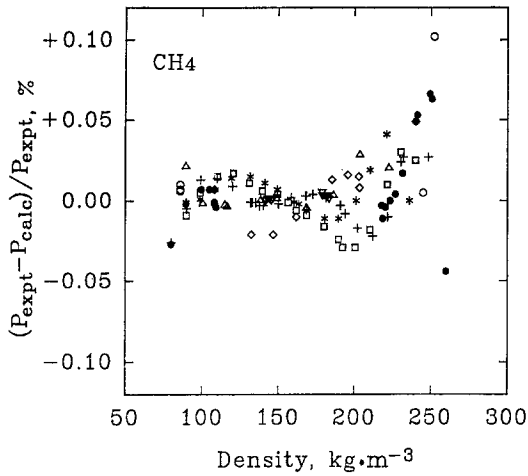

Fig. 1. Percentage deviations of the experimental pressures [13–15] from the crossover equation of state. ○, $T=186.012$ K; ●, $T=189.012$ K; ▽, $T=190.512$ K; +, $T=190.567$ K; □, $T=193.012$ K; ∗, $T=196.011$ K; △, $T=200.011$ K; ◇, $T=207.010$ K.

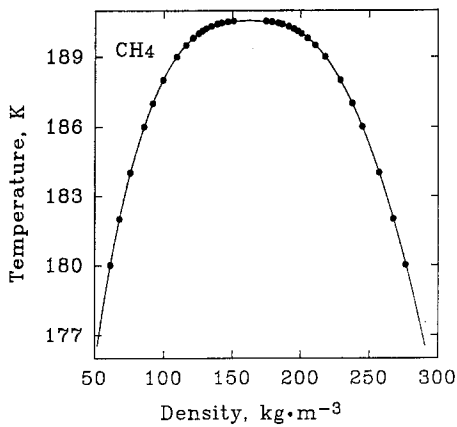

Fig. 2. Coexisting vapor and liquid densities as a function of temperature. The solid curve represents the coexistence curve calculated from the crossover equation of state. The data points represent experimental values reported by Kleinrahm and Wagner [13].

The deviations of the experimental pressure data from our equation in this range are shown in Fig. 1. Our crossover equation is based on a theoretical match-point solution, which is exact for $M=0$, but which becomes less accurate for $M \neq 0$, i.e., for densities smaller or larger than the critical density [19, 21]. From Fig. 1 we note that our crossover equation does slightly better at the low-density side than at the high-density side. A comparison between the coexistence boundary as implied by our crossover equation of state and the experimental saturated densities is presented in Fig. 2; the corresponding deviations are within the experimental uncertainty. A comparison between the vapor pressures calculated from our crossover equation of state and the experimental vapor pressures is presented in Fig. 3; the deviations are smaller than 0.01 %.

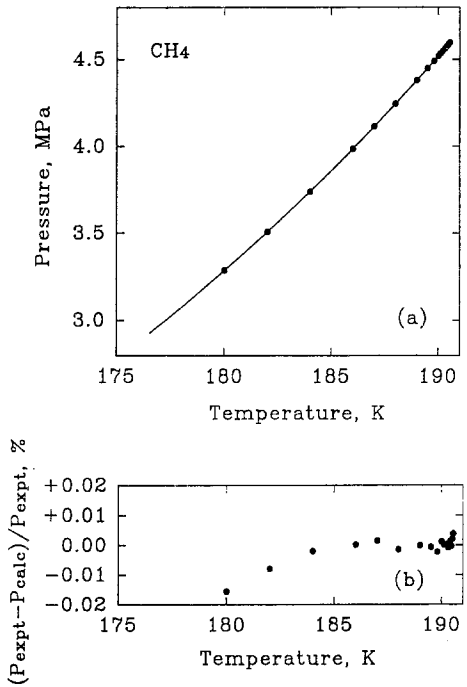

Fig. 3. (a) The vapor pressures as a function of temperature. The solid curve represents the vapor pressures calculated from the crossover equation of state. The data points represent experimental values reported by Kleinrahm and Wagner [13]. (b) Percentage deviations of the experimental vapor pressures.

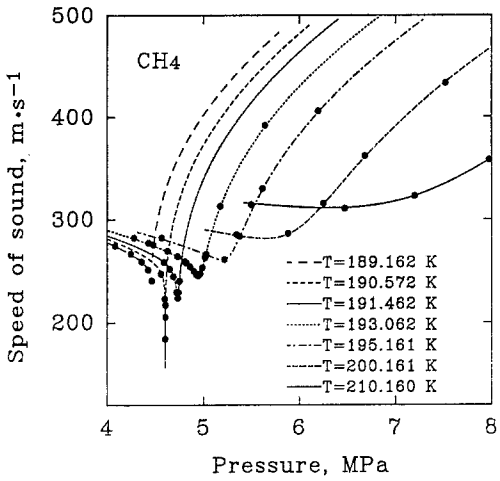

Fig. 4. Sound velocity at selected temperatures as a function of pressure. The curves represent the values calculated from the crossover model. The data points represent experimental data reported by Gammon and Douslin [24] and Sivaraman and Gammon [25].

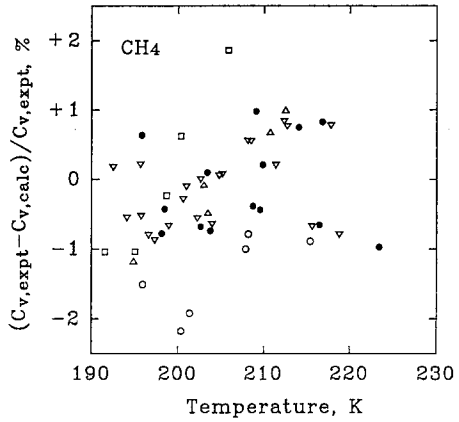

Fig. 5. Percentage deviations of the experimental isochoric specific-heat data [26, 27] from the crossover model. ○, $\rho = 128.7 - 128.9\ \text{kg} \cdot \text{m}^{-3}$; ●, $\rho = 163.2 - 163.5\ \text{kg} \cdot \text{m}^{-3}$; ▽, $\rho = 189.0 - 189.9\ \text{kg} \cdot \text{m}^{-3}$; △, $\rho = 216.2 - 216.6\ \text{kg} \cdot \text{m}^{-3}$; □, $\rho = 231.1 - 231.5\ \text{kg} \cdot \text{m}^{-3}$.

Table III. Table for Checking Computer Programs

Temperature (K)	Density ($kg \cdot m^{-3}$)	Pressure (MPa)	c_V ($kJ \cdot kg^{-1} \cdot K^{-1}$)	c_P ($kJ \cdot kg^{-1} \cdot K^{-1}$)	Speed of sound ($m \cdot s^{-1}$)	Phase region
187.00	120.00	4.114	8.370			II
189.00	120.00	4.380	9.360			II
191.00	120.00	4.618	2.650	50.86	245.5	I
193.00	120.00	4.830	2.471	30.62	255.1	I
187.00	160.00	4.114	7.018			II
189.00	160.00	4.380	7.760			II
191.00	160.00	4.662	3.394	595.0	213.1	I
193.00	160.00	4.949	2.664	81.14	246.3	I
187.00	200.00	4.114	6.206			II
189.00	200.00	4.380	6.799			II
191.00	200.00	4.703	2.516	52.46	265.1	I
193.00	200.00	5.085	2.343	29.27	289.1	I

The caloric background coefficients $\tilde{\mu}_j$ for $j \geqslant 2$ were determined from the experimental sound-velocity data reported by Gammon and Douslin [24] and Sivaraman and Gammon [25] and the specific-heat data of Younglove [26] as corrected by Roder [27]. In Fig. 4, we show the sound velocity as a function of pressure at a number of temperatures; the good agreement between experimental and calculated sound velocities is evident. We should mention that we did not include in this comparison sound-velocity data near the phase boundary, since they seem to be appreciably less accurate than those in the one-phase region away from the phase boundary [9, 24, 25]. The deviations of the experimental c_V data from our equation are shown in Fig. 5. Our crossover equation for the Helmholtz free-energy density reproduces the sound-velocity and specific-heat data with a standard deviation of 0.8%.

The coefficients $\tilde{\mu}_0$ and $\tilde{\mu}_1$ determine the zero points of entropy and energy. These coefficients were fixed by matching our equation with the global equation of Setzmann and Wagner at a reference point selected at $T = 220$ K and $\rho = 160\ kg \cdot m^{-3}$. Values calculated for the pressure, specific heats, and sound velocity at a few selected temperatures and densities as an aide for checking computer programs are presented in Table III.

4. COMPARISON WITH THE EQUATION OF SETZMANN AND WAGNER

Our crossover equation for the Helmholtz free-energy density yields a representation of the thermodynamic properties of methane equivalent to

or better than the analytic equation of Setzmann and Wagner [12] in an approximately triangular region in the temperature–density plane bounded by the lines

$$T = 186.2$$
$$T = +0.417\rho + 266.52 \tag{15}$$
$$T = -0.457\rho + 282.37$$

where T is in K and ρ is in $\mathrm{kg \cdot m^{-3}}$. This region is shown in Fig. 6 and can be subdivided into two regions, I and II, also shown in Fig. 6. In region I the sound velocities, isochoric specific heats, and isobaric specific heats calculated from our crossover equation and from the equation of Setzmann and Wagner differ by less than 1%. Hence, in this region one can switch from our crossover equation to the analytic equation of Setzmann and Wagner without significant jumps in any of the thermodynamic properties.

In region II the differences between our nonanalytic equation and the analytical equation become significant. While the equation of Setzmann and Wagner does represent the actual experimental specific-heat data for methane, it implies a finite c_V of about $3.6 \times 10^3\ \mathrm{kJ \cdot kg^{-1} \cdot K^{-1}}$ at the

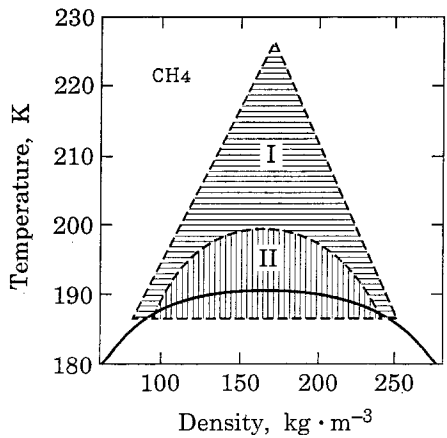

Fig. 6. Recommended range for the crossover model. In region I the calculated sound velocity, isochoric specific heat, and isobaric specific heat agree with the analytic equation of Setzmann and Wagner within 1%. In region II the nonanalytic and analytic equation yield different results. The solid curve represents the two-phase boundary.

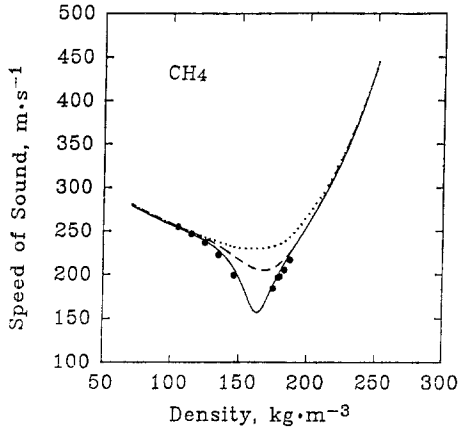

Fig. 7. The sound velocity as a function of density at $T = 190.572$ K. The solid curve represents the crossover model, the dashed curve the analytic equation of Setzmann and Wagner [12] and the dotted curve the analytic equation of Friend et al. [11]. The data points represent experimental data reported by Gammon and Douslin [24].

critical point, while the critical scaling laws imply a divergent c_V. The experimental sound-velocity data are sufficiently close to the critical point so that the difference between our nonanalytic equation and the global analytic equation becomes visible as shown in Fig. 7. In this figure we also show the sound velocity calculated from the global analytic equation of Friend et al. [11]. The scaling laws imply that the sound velocity vanishes at the critical point, while the analytic equations fail to follow the rapid decrease of the sound velocity in the near vicinity of the critical point.

ACKNOWLEDGMENTS

We are indebted to W. Wagner for valuable discussions and for providing us with Refs. 12 and 15 prior to publication and to J. C. Rainwater for a critical reading of the manuscript. One of us (J.V.S.) also acknowledges the hospitality of G. M. Schneider at the Ruhr-Universität Bochum, where the paper was completed. The research was supported by the Division of Chemical Sciences of the Office of Basic Energy Sciences of the U.S. Department of Energy under Grant DE-FG05-88ER13902.

REFERENCES

1. M. Levy, J. C. Le Guillou, and J. Zinn-Justin (eds.), *Phase Transitions: Cargèse 1980* (Plenum, New York, 1981).
2. J. V. Sengers and J. M. H. Levelt Sengers, *Int. J. Thermophys.* **5**:195 (1984).
3. J. V. Sengers and J. M. H. Levelt Sengers, *Annu. Rev. Phys. Chem.* **37**:189 (1986).
4. F. W. Balfour, J. V. Sengers, M. R. Moldover, and J. M. H. Levelt Sengers, in *Proceedings of the 7th Symposium on Thermophysical Properties*, A. Cezairliyan, ed. (American Society of Mechanical Engineers, New York, 1977), p. 786; *Phys. Lett.* **65A**:223 (1978).
5. G. A. Chapela and J. S. Rowlinson, *J. Chem. Soc. Faraday Trans. I* **70**:584 (1974).
6. S. Angus, B. Armstrong, K. M. de Reuck, V. V. Altunin, V. V. Gadetskii, G. A. Chapela, and J. S. Rowlinson, *International Thermodynamic Tables of the Fluid State—3. Carbon Dioxide* (Pergamon, New York, 1976).
7. H. W. Woolley, *Int. J. Thermophys.* **4**:51 (1983).
8. S. Angus, B. Armstrong, and K. M. de Reuck, *International Thermodynamic Tables of the Fluid State—5. Methane* (Pergamon, New York, 1978).
9. D. S. Kurumov, G. A. Olchowy, and J. V. Sengers, *Int. J. Thermophys.* **9**:73 (1988).
10. V. Brandani and J. M. Prausnitz, *J. Phys. Chem.* **85**:3207 (1981).
11. D. G. Friend, J. F. Ely, and H. Ingham, *J. Phys. Chem. Ref. Data* **18**:583 (1989).
12. U. Setzmann and W. Wagner, *J. Phys. Chem. Ref. Data* **20**:1 (1991).
13. R. Kleinrahm and W. Wagner, *J. Chem. Thermodynam.* **18**:739 (1986).
14. R. Kleinrahm, W. Duschek, and W. Wagner, *J. Chem. Thermodynam.* **18**:1103 (1986).
15. G. Händel, R. Kleinrahm, and W. Wagner, *J. Chem. Thermodynam.* (in press).
16. J. V. Sengers and J. M. H. Levelt Sengers, in *Progress in Liquid Physics*, C. A. Croxton, ed. (Wiley, New York, 1978), p. 103.
17. Z. Y. Chen, A. Abbaci, and J. V. Sengers, in *Properties of Water and Steam, Proceedings of the 11th International Conference*, M. Píchal and O. Šifner, eds. (Hemisphere, New York, 1990), p. 168.
18. Z. Y. Chen, A. Abbaci, S. Tang, and J. V. Sengers, *Phys. Rev. A* **42**:4470 (1990).
19. S. Tang, J. V. Sengers, and Z. Y. Chen, *Physica A* **179**:344 (1991).
20. J. F. Nicoll, *Phys. Rev. A* **24**:2203 (1981).
21. Z. Y. Chen, P. C. Albright, and J. V. Sengers, *Phys. Rev. A* **41**:3161 (1990).
22. M. L. McGlashan, *J. Chem. Thermodynam.* **22**:653 (1990).
23. M. Ley-Koo and M. S. Green, *Phys. Rev. A* **16**:2483 (1977).
24. B. E. Gammon and D. R. Douslin, *J. Chem. Phys.* **64**:203 (1976).
25. A. Sivaraman and B. E. Gammon, *Speed-of-Sound Measurements in Natural Gas Fluids*, Gas Research Institute Report 86/0043 (Gas Research Institute, Chicago, 1986).
26. B. A. Younglove, *J. Res. Natl. Bur. Stand. (USA)* **78A**:401 (1974).
27. H. M. Roder, *J. Res. Natl. Bur. Stand. (USA)* **80A**:739 (1976).